Engineering Fracture Mechanics Vol. 29, No. 6, pp. 683–696, 1988
Printed in Great Britain.

0013-7944/88 $3.00 + .00

A STRUCTURAL APPROACH TO THE CALCULATION OF J

R. BRADFORD
Operational Engineering Division, CEGB, Bristol, U.K.

Abstract—The calculation of the elastic–plastic fracture parameter, J, is often assumed to demand finite element analysis, particularly when the loads applied are secondary, or partly secondary, in nature, e.g. thermal load. However, it is shown that a simple technique based on the reference stress approach can be used to calculate J even in these cases. Example results are given, and compare well with finite element solutions.

INTRODUCTION

IT IS GENERALLY held at the present time that the parameter J of Eshelby[1] and Rice[2] forms the best means of assessing the likelihood of ductile fracture. Thus, the practising engineering, in attempting to decide on the acceptability of a given level of cracking, is left with the problem of calculating J. In the case of linear behaviour and simple geometries, the task of calculating the stress intensity factor (and hence J) is aided by the existence in the literature of many 'standard' solutions. In a similar way, Kumar, German and Shih[3] have given J-estimation schemes in the non-linear case for a limited range of geometries and stress–strain behaviours. A more general method of approximating J has been given by Ainsworth *et al.*[4], and included in the CEGB's R6 defect assessment methodology[5].

The most general, and potentially the most accurate, technique for calculating J is the finite element method. Facilities to perform finite element analyses are now widely available to engineers, at least as regards elastic analyses. As for elastic–plastic FE analysis, although a great many useful results have been obtained, the method is still more appropriate to a research environment than an engineering environment. This is particularly true beyond general yield and/or in three dimensions when the problem becomes computationally heavy and may not converge. Consequently, simple J-estimation procedures such as that of [4] are of considerable importance. The main shortcoming of this method is that is it applicable only in load controlled situations in which an appropriate 'reference stress' is known.

Two types of situation arise in which the reference stress is not known. Firstly, the loading may be secondary or partly secondary in nature, e.g. applied displacements or thermal strains. The second possibility, which is really a special case of the first, occurs when the stresses at the crack location arise due to the requirement of displacement compatibility. In this work we shall describe how J may be calculated for these cases. The general procedure is described in the next section, and the following sections give examples of the method when applied to problems of both the above types.

METHOD OF J ESTIMATION

We firstly describe the method of Ainsworth *et al.*[4] for the load controlled case. This method assumes that;
(a) a solution is available for the linear elastic stress intensity factor, K, and,
(b) a limit-load solution is known for the cracked body, giving the value of the load, F_y, when the remaining uncracked ligament generally yields. (Note: F is merely symbolic for whatever type of loads are acting).

A reference stress, σ, is then defined by,

$$\sigma = (F/F_y)\sigma_y,\ \sigma_y = 0.2\%\ \text{proof stress} \tag{1}$$

and the elastic–plastic J is approximated by,

$$J = A(\sigma)K^2/E \tag{2}$$

where K is evaluated at the same load, F, as that for which J is required. The reference stress function is,

$$A(\sigma) = \frac{E\epsilon}{\sigma} + \frac{\sigma^3}{2E\epsilon\sigma_y^2} \tag{3}$$

where E = Young's Modulus, and ϵ is the true uniaxial strain corresponding to a true uniaxial stress of magnitude σ. Note that eq. (2) applies to plane stress. For plane strain the RHS of (2) should be multiplied by $(1-\nu^2)$, ν = Poisson's ratio.

We now show how the preceding J-estimation scheme can be used to find the (generalized) displacement corresponding to the applied loads, provided that these displacements are known (or negligible) in the uncracked case. For purposes of illustration we shall assume a point load, P, and a moment, M, conjugate to a displacement, D, and a rotation, θ. The complementary energy is,

$$U = \int D\,\mathrm{d}P + \int \theta\,\mathrm{d}M \tag{4}$$

and the energy-rate interpretation of J gives,

$$J = \frac{\delta U}{\delta S} \tag{5}$$

where S is the crack area, and the derivative is carried out at constant loads, P and M. Appropriate differentiation and integration of eqs (4) and (5) gives,

$$D(S) = D(0) + \int_0^S \frac{\delta J}{\delta P}\,\mathrm{d}S \tag{6}$$

$$\theta(S) = \theta(0) + \int_0^S \frac{\delta J}{\delta M}\,\mathrm{d}S \tag{7}$$

where all the terms are evaluated at the same loads, P and M. The derivative in (6) is taken at constant M, and that in (7) at constant P. These equations give the displacement/rotation of the cracked body for a crack of size S. The first terms on the RHS are the corresponding uncracked quantities which must be calculated separately. In many cases, the uncracked body would respond linearly (i.e. yielding is confined to the ligament) and this simplifies the calculation of $D(0)$, $\theta(0)$. The integral terms in (6, 7) give the extra displacement/rotation due to the presence of the crack, including the effects of plasticity on the ligament.

Thus, eqs (6, 7) give the (generalized) displacements for a given load level. Since (2) gives J for a given load, this allows J to be found at a specified displacement. The following sections illustrate the use of this technique in several example problems.

CENTRE CRACKED PLATE

The geometry for this problem is shown in Fig. 1. The plate is subjected to a thermal load which consists of heating the outer edges, thereby causing the inner (cracked) part to be in tension. In addition, a uniform tensile stress is applied at the ends of the plate. The assumed material data is given in Fig. 2. The coefficient of linear expansion is $\alpha = 12 \times 10^{-6}/°C$. Both the mechanical and the thermal load, if applied alone to the uncracked body, would give rise to stresses of σ_0, ie. the proportionality limit stress.

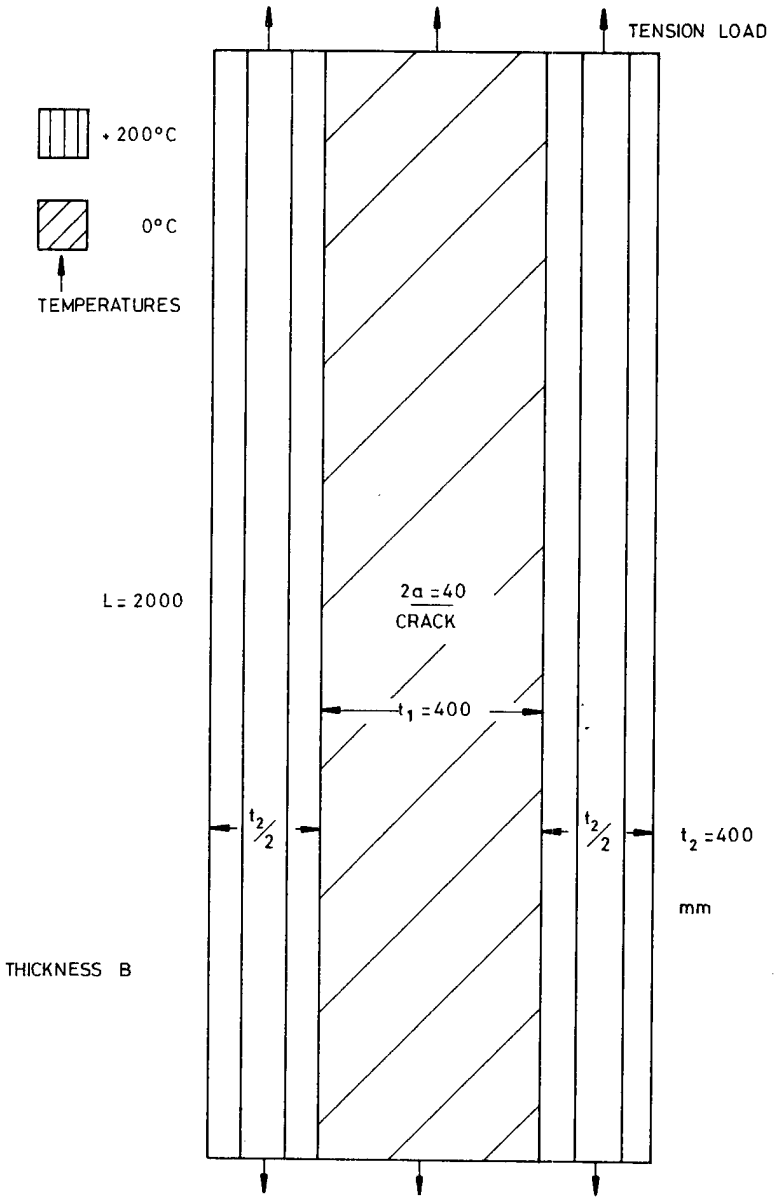

Fig. 1. Centre-cracked plate geometry showing the temperature distribution and the mechanical tensile load.

To facilitate the analysis, the actual problem is replaced by a simplified problem in which the hot and cold regions are treated as separate plates. The latter are assumed connected at their ends to a rigid cross-beam, so that the extension (D) of each is the same. Thermal loading is thus transmitted to the central part as simple tension, rather than shear across the hot–cold interface as is actually the case. For small cracks, where the compliance factor is little larger than unity, this idealization is probably reasonable. Clearly it will be grossly in error when $2a \geqslant t_1$.

We now develop the theory for this simplified problem using the following notation:

C_1 = current (tangential) stiffness of central part,
C_2 = current (tangential) stiffness of outer parts (sum of both),
D = common displacement of all parts,
F = total force on beam = $F_1 + F_2$,
F_1 = load currently carried by the central part,
F_2 = load currently carried by the outer parts (sum of both).

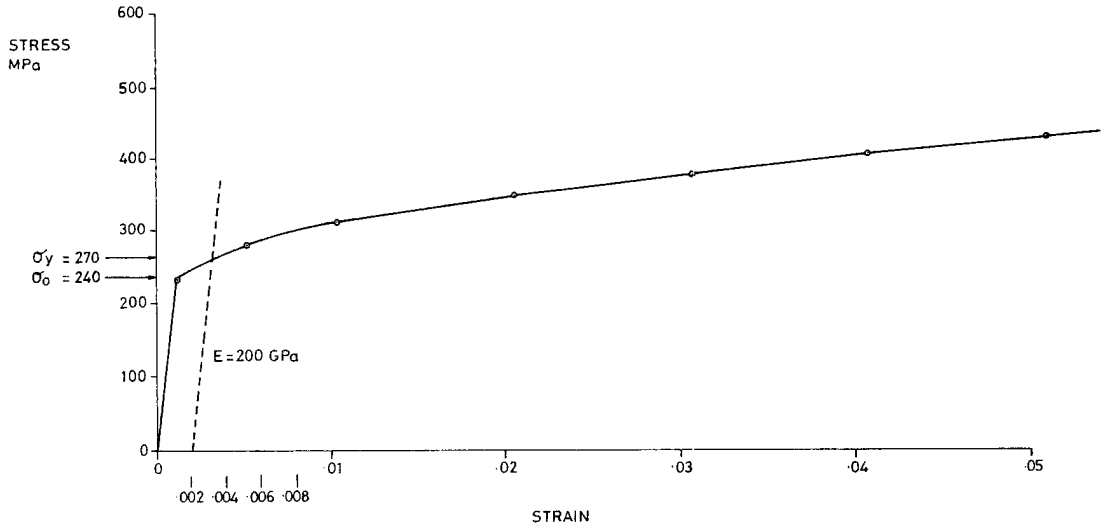

Fig. 2. Stress–strain data employed.

Remembering that the outer parts may expand due to an applied temperature change (ΔT), we have,

$$\Delta F_1 = C_1 \Delta D \tag{8}$$

$$\Delta F_2 = C_2(\Delta D - \alpha L \Delta T) \tag{9}$$

where Δ denotes a small change. For the outer parts, the tangential stiffness is simply the slope of the material stress–strain curve, suitably normalized,

$$C_2 = \frac{Bt_2}{L}\left(\frac{d\sigma}{d\epsilon}\right)_2 \tag{10}$$

where the subscript denotes evaluation at the current stress ($\sigma_2 = F_2/Bt_2$) in the outer parts.

In the case of the central region, the tangential stiffness must depend upon the crack length. From the general theory developed above it is clear that differentiation of an equation like (6) with respect to load will give the tangential flexibility (reciprocal of tangential stiffness). For the present problem this gives,

$$\frac{1}{C_1(a)} = \frac{1}{C_1(a=0)} + 2B\int_0^a \frac{\delta^2 J}{\delta F_1^2}\,da \tag{11}$$

where $C_1(a=0)$ is the uncracked tangential stiffness evaluated at the same load (F_1) as $C_1(a)$ and is given by an expression similar to (10), i.e.

$$C_1(a=0) = \frac{Bt_1}{L}\left(\frac{d\sigma}{d\epsilon}\right)_1 \text{ (evaluated at } \sigma_1 = F_1/Bt_1). \tag{12}$$

J is the "energy rate" for the *central part alone*,

$$J = \frac{1}{2B}\left(\frac{\delta u}{\delta a}\right) \text{constant } F_1,\ u = \int D\,dF_1 \tag{13}$$

and is known in terms of the central load, F_1, from eqs (2, 3). In this case, we use, for the reference stress,

$$\sigma = \frac{\sigma_1}{\left(1 - \frac{2a}{t_1}\right)} \tag{14}$$

and for the stress intensity (K) we use a standard solution for a centre-cracked plate of width t_1, which, for $2a/t_1 = 0.1$ gives,

$$K = 1.005\sigma_1\sqrt{\pi a}\,. \tag{15}$$

Finally, adding equations, (8) and (9) gives,

$$(C_1 + C_2)\Delta D = \Delta F + \alpha L C_2 \Delta T. \tag{16}$$

Hence, since C_1 and C_2 are known in terms of the current stress state, ΔD may be found for any specified load increment (i.e. given ΔF and ΔT). The stress increments, $\Delta\sigma_1$, and $\Delta\sigma_2$, are then found from eqs (8) and (9).

The results are plotted in Figs 3 and 4, essentially giving J as a function of applied load. The load has been normalized as,

$$L_r = \frac{\sigma_0(f_1 + f_2)}{\sigma_y\left(1 - \frac{2a}{t_1}\right)} \tag{17}$$

where f_1 and f_2 are the fractions of the total mechanical and thermal load applied. Similarly, the ordinate is the dimensionless quantity,

$$K_r = \left[\frac{J(\text{elastic})}{J(\text{elastic–plastic})}\right]^{1/2}. \tag{18}$$

For comparison, the R6 assessment diagram[5] is also included in Figs 3 and 4. More importantly, these figures also include the results of a finite element analysis of the same problem due to Muscati[6]. The agreement between the finite element results and the present method is

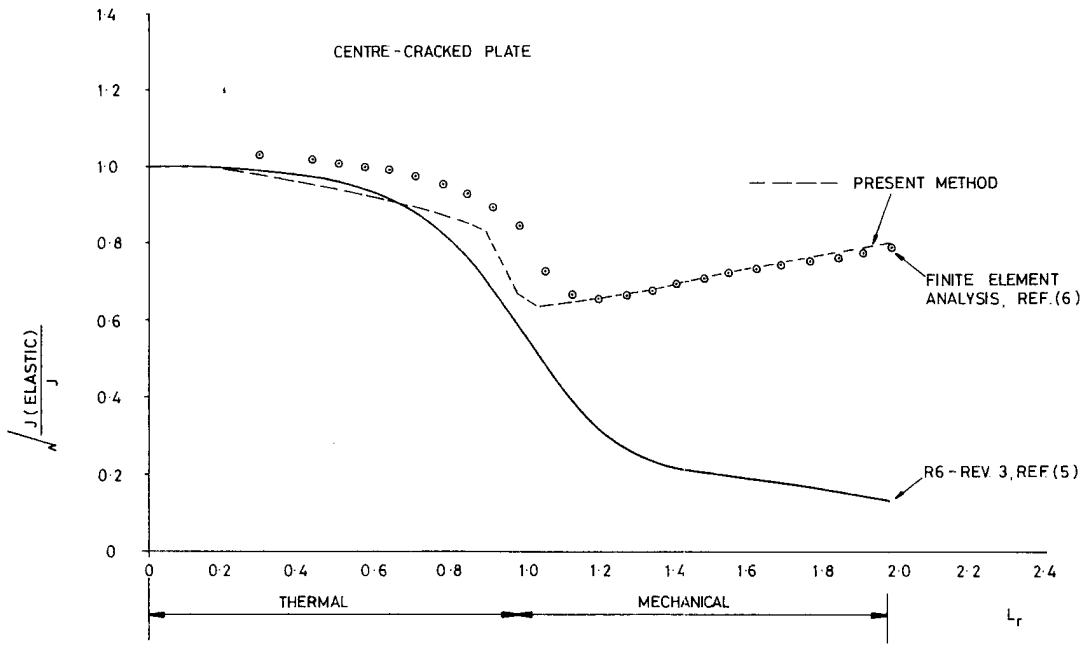

Fig. 3. Results plotted in *R6* format thermal-then-mechanical (nominal applied stresses σ_0).

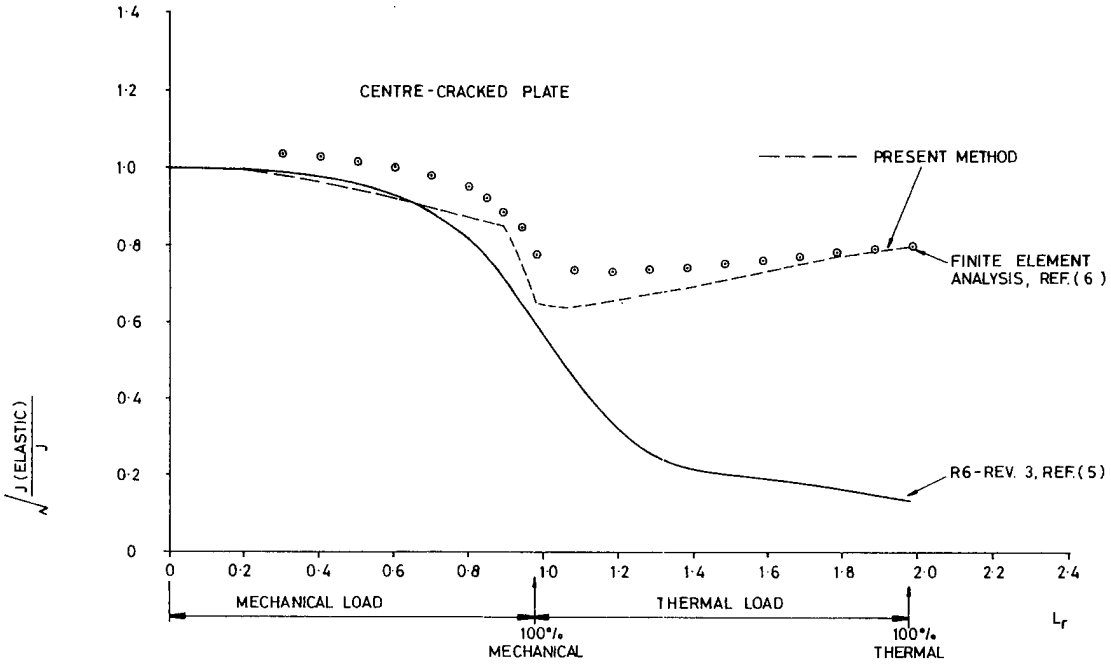

Fig. 4. Results plotted in *R6* format mechanical-then-thermal (nominal applied stresses σ_0).

good, particularly at the highest loads. The reference stress method errs on the conservative side, i.e. overestimates J. At the full (mechanical + thermal) load, the unnormalized results for the elastic–plastic stress intensity, i.e. $\sqrt{EJ}$, are as shown in Table 1. In passing we note that at applied load levels higher than σ_0, the reference stress method gives a clear prediction of a load-order dependence. This is illustrated in Table 1 for the case when the nominal (plastic) stress which would arise due to either load separately is raised to σ_y.

CIRCUMFERENTIALLY CRACKED CYLINDER

In this example, a thin cylinder containing a fully circumferential uniform, internal crack is subjected to an axial tensile stress and, simultaneously, a thermal load. The latter consists of a linear, axial temperature distribution, increasing from zero at a symmetry plane where the internal circumferential crack is introduced, see Fig. 5. If the symmetry condition ($U_z = 0$ on $z = 0$) were relaxed, then zero stresses would result and the deformation would be as shown in Fig. 5. Thus, the thermal load can be considered (at least for a *thin* cylinder) as equivalent to an applied rotation of $\theta = \alpha\beta r$ at the symmetry plane. When this plane is cracked, the rotation applies to the ligament only, and hence corresponds to a smaller bending moment (M). Note:

α = coefficient of linear expansion,
β = axial temperature gradient,
r = mean cylinder radius = $(r_i + r_0)/2$,
$t = r_0 - r_i$ = thickness,
M = moment per unit circumference ($2\pi r$),
N = force per unit circumference.

Table 1. Full load results for centre cracked plate

Method	Nominal stress	Mechanical then thermal	Thermal then mechanical
Finite Elements (ref. [6])	σ_0	152.3	153.5
Present method	σ_0	151.0	150.7
Present method	σ_y	267.1	211.8

Values are for $\sqrt{EJ}$, MPa$\sqrt{m}$.

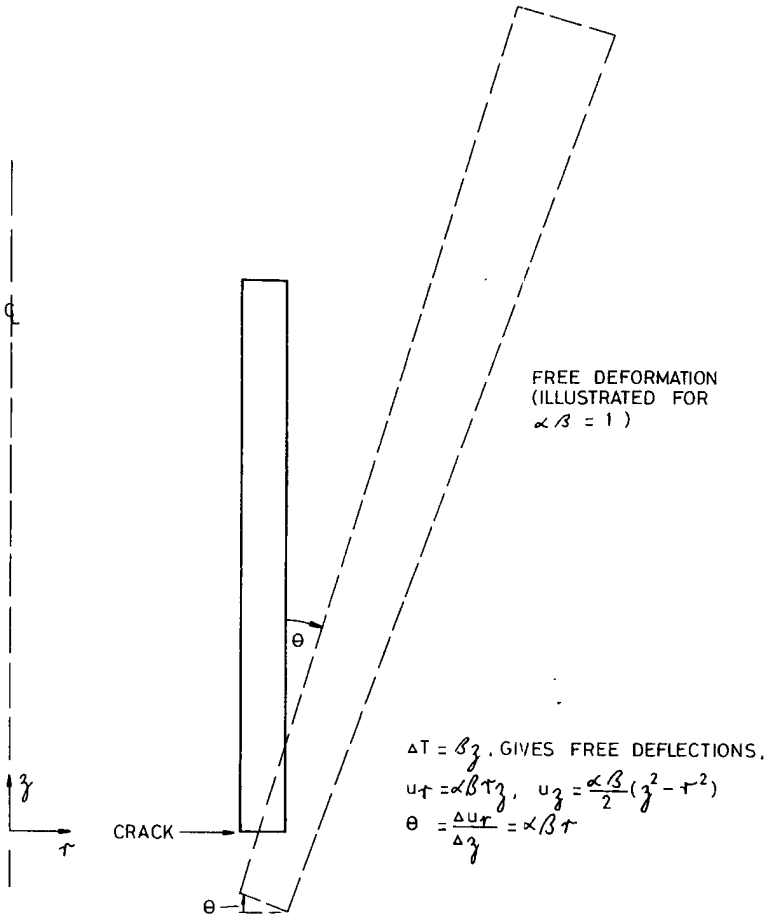

Fig. 5. Geometry and thermal load (for cylinder).

This problem has also been analysed by Muscati[6] using the finite element method. To allow comparison, we use the same numerical data,

$$r = 500, \quad t = 50, \quad \text{half-length} = 1250\,\text{mm}$$

$$\alpha = 46 \times 10^{-6}/°\text{C}, \text{ crack depth, } a = 18.6\,\text{mm} \ (a/t = 0.372)$$

whilst the stress–strain data is the same as for the previous problem (Fig. 2).

The magnitude of the applied thermal load, β, specifies the equivalent rotation, θ. However, the reference stress formula for J, (2), applies only for a known load, so that the problem is to find M. This is accomplished using equation (7), which in the present case reads,

$$\theta(a, M, N) = \theta(0, M, N) + \int_0^a \frac{\partial J}{\partial M} \mathrm{d}a \tag{19}$$

where the derivative $\partial J/\partial M$ is carried out at constant tension (N) and crack depth (a). Thus, eq. (19) allows the moment-rotation behaviour to be found, so long as the uncracked response is known. Note that, since J depends upon N as well as M, θ will also depend upon both loads. Thus, for a given thermal load (i.e. a fixed θ), applying a small amount of tension (N) leads to a decrease of bending moment, M.

For simplicity we shall assume that the loads M and N which act on the ligament are restricted to values for which the uncracked cylinder would respond linearly. The standard solution for a semi-infinite cylinder is then,

Table 2. LEFM Compliance factors (cylinder)

a/t	k_m	k_b
0	1.122	1.122
0.1	1.157	1.012
0.2	1.252	0.957
0.3	1.390	0.924
0.4	1.570	0.890
0.5	1.780	0.890
0.6	2.025	0.941

$$\theta(0, M, N) = \frac{M}{D\lambda}, \quad \lambda = \left[\frac{3(1-\nu^2)}{r^2t^2}\right]^{1/4}, \quad D = \frac{Et^3}{12(1-\nu^2)} \tag{20}$$

(independent of N).

To find J for given loads N and M we require K and reference stress values for substitution into eqs (2, 3). For the former we use,

$$K_m = k_m\sigma_m\sqrt{\pi a}, \qquad \sigma_m = \frac{N}{t} \tag{21}$$

$$K_b = k_b\sigma_b\sqrt{\pi a}, \qquad \sigma_b = \frac{6M}{t^2} \tag{22}$$

$$K = K_m + K_b \tag{23}$$

where the compliance factors are given in Table 2. We are interested in the case of a dominant thermal (bending) load, with a relatively small tension. An appropriate limit solution gives a reference stress,

$$\sigma = \frac{1.09q(2M+Nt)t^2}{(t-a)^2(t^2+1.686at-2.72a^2)} \tag{24}$$

where the parameter q varies according to the relative amount of bending and tension, and is given in Table 3. Thus, we can now calculate the moment–rotation curves, as shown in Fig. 6, for specified tensile loads.

Figure 7 plots J against load, firstly for a thermal load up to 1°C/mm, and then an axial tension applied whilst the thermal load is held constant at 1°C/mm. Note that general yielding at a level of σ_0 occurs at a thermal load of about 0.5°C/mm. Figure 7 also shows the finite element results of Muscati[6], which are in good agreement with the present results, differing by only ~3% in J at 100% thermal load. Moreover, the increase in J caused by the subsequent tension

Table 3. q-Function for limit solution

y†	q
0	1.588
0.1	1.4
0.2	1.2
0.32	1.0
0.4	0.9
0.485	0.795
0.55	0.732
0.61	0.72
0.68	0.743
0.788	0.81
1.0	1.0

†$y = \left(1-\frac{a}{t}\right)\Big/\left(1+\frac{2M}{Nt}\right)$.

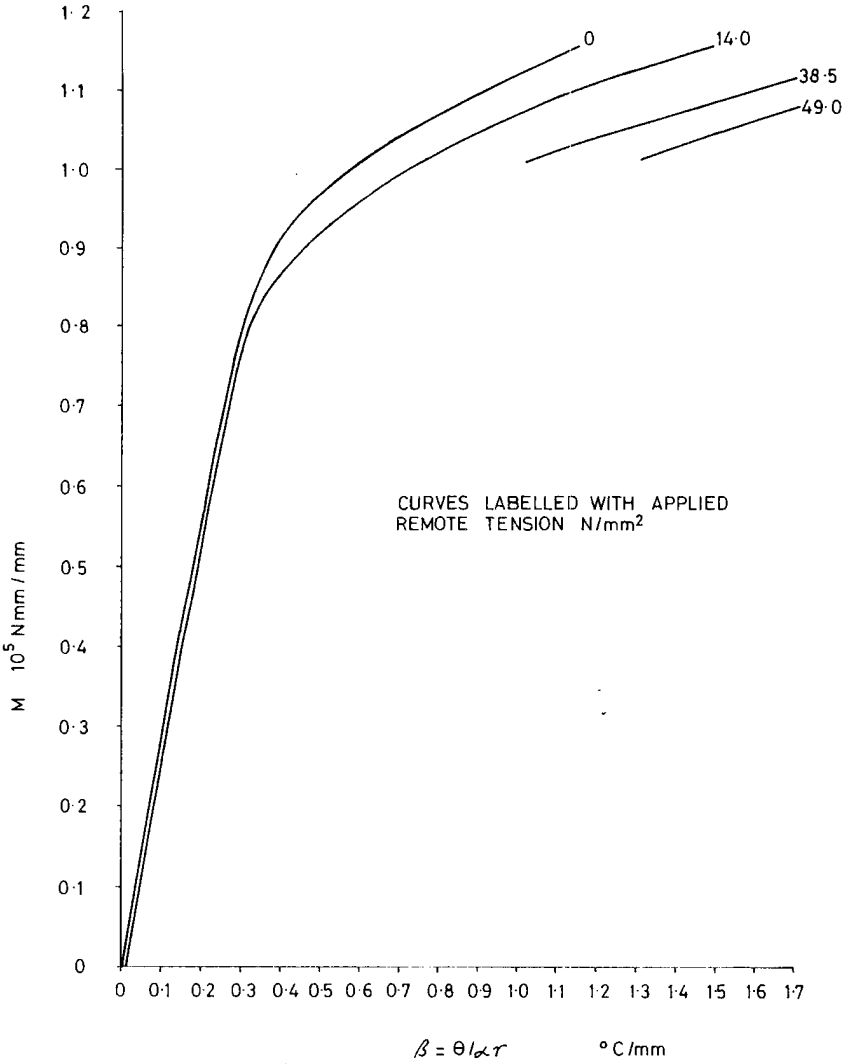

Fig. 6. Bending moment at ligament vs applied thermal gradient (cylinder).

is consistent between the two methods. This is noteworthy since the bending moment, M, is known to fall as a result of applying the tension at fixed β (see Fig. 6), so that the change in J is a result of the competition between increasing N and decreasing M. Numerical results for J are given in Table 4. It is of interest that reasonable agreement (4%) is obtained in the elastic regime, since, even in this case, the crack causes a substantial increase in the flexibility [i.e. the second term in eq. (19) is significant].

BEAM CRACKED AT BOTH BUILT-IN ENDS

The geometry for this final example is shown in Fig. 8(a). Cracks of depth a exist on the top surfaces of both ends of a beam of length l, loaded by a point load of $2F$ in its centre. The uncracked ligaments are subject to bending and shear stresses, as shown in Fig. 8(b). Yielding is assumed to be confined to a small region around the ligaments, i.e. in Fig. 8(b) the limit $h \to 0$ is to be understood. The elastic response of the rest of the beam produces a rotation at the ends of,

$$\theta = \alpha F - \beta M \tag{25}$$

where

$$\alpha = \frac{3l^2}{2EBt^3}, \quad \beta = \frac{6l}{EBt^3}. \tag{26}$$

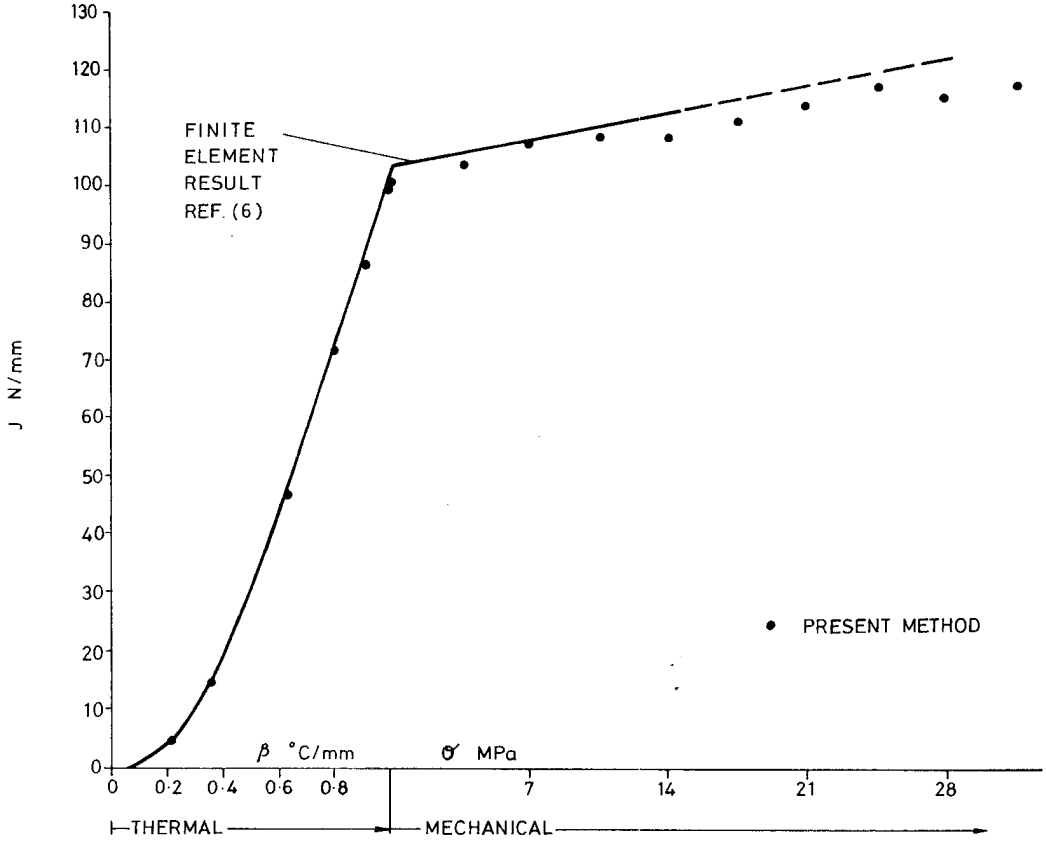

Fig. 7. Comparison of finite element results and present method.

This must be compatible with the elastic–plastic rotation of the vanishingly small regions of length h, whose rotation is given by eq. (7). In this case, the limit $h \to 0$ ensures that the uncracked term is zero. Hence, equating (7) and (25) gives,

$$\frac{M}{F} = \frac{\alpha}{\beta + \dfrac{B}{M}\displaystyle\int \frac{\partial J}{\partial M}\,\mathrm{d}a}. \tag{27}$$

Because the stressing is mixed-mode, the stress intensity for substitution into eq. (2) is,

Table 4. Comparison of J resulting from present method and finite elements[6] (cylinder)

Thermal load β °C/mh	Applied tension MPa	J N/mm Present method	J N/mm Finite elements[6]	% Difference
0.05	0	0.263	0.274	4.0
0.15	0	2.409	2.480	2.9
0.35	0	14.49	15.34	5.5
0.65	0	52.0	51.65	−.7
0.75	0	64.9	65.9	1.5
0.85	0	78.0	80.7	3.4
0.95	0	92.2	95.9	3.9
1.0	0	100.3	103.7	3.3
1.0	3.5	103.0	105.8	2.7
1.0	7	106.3	108.0	1.6
1.0	10.5	107.6	110.2	2.3
1.0	14	107.4	112.4	4.4

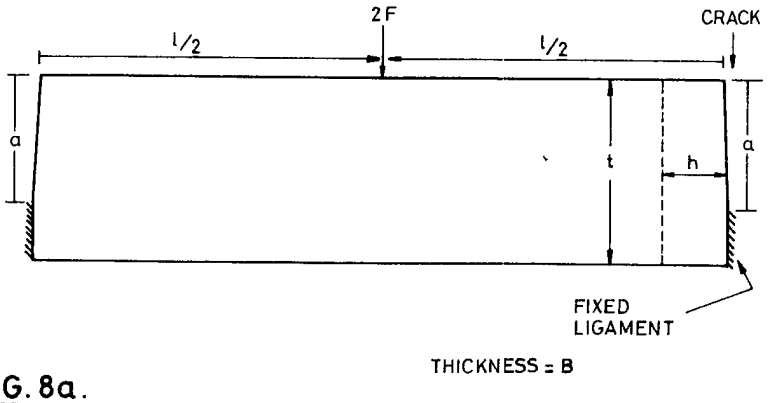

FIG. 8a.

GEOMETRY OF BEAM

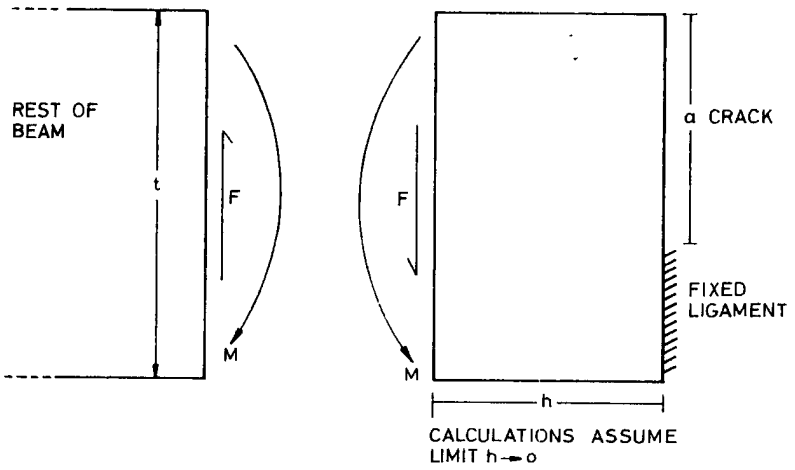

FIG. 8b.

Fig. 8. (a, b) Geometry of beam.

$$K^2 = K_{\mathrm{I}}^2 + K_{\mathrm{II}}^2, \tag{28}$$

where

$$K_{\mathrm{I}} = k_{\mathrm{I}} \frac{6M}{Bt^2} \sqrt{\pi a} \tag{29}$$

$$K_{\mathrm{II}} = k_{\mathrm{II}} \frac{F}{Bt} \sqrt{\pi a} \tag{30}$$

and the compliance factors, k_{I} and k_{II}, are given in Table 5. For the limit load we use, for illustration, a plane strain, upper bound Mises solution, which gives a reference stress,

$$\sigma = \left[\left(\frac{2.75M}{B(t-a)^2} \right)^2 + 3 \left(\frac{F}{B(t-a)} \right)^2 \right]^{1/2}. \tag{31}$$

Table 5. Elastic compliance factors (beam)

a/t	k_b	k_{II}‡
0	1.122	1.0
0.05	1.070	1.001
0.1	1.045	1.004
0.15	1.041	1.009
0.2	1.054	1.017
0.25	1.08	1.027
0.3	1.123	1.040
0.35	1.182	1.056
0.4	1.255	1.075
0.45	1.36	1.099
0.5	1.50	1.128
0.55	1.673	1.164
0.6	1.91†	1.208
0.65	2.25	1.264
0.7	2.73	1.336
0.75	3.46	1.432
0.8	4.69	1.565
0.85	7.0	1.766
0.9	12.5	2.113
0.95	34.4	2.918
0.99	377	6.4

†Asymptotic value $\dfrac{0.375}{\left(\frac{c}{t}\right)^{1/2}\left(1-\frac{c}{t}\right)^{3/2}}$.

‡ $\left[\dfrac{2t}{\pi a}\tan\dfrac{\pi a}{2t}\right]^{1/2}$.

Thus, eqs (28–31) allow J to be found from eqs (2, 3) for given M and F. Substitution into eq. (27) therefore produces an equation which implicitly gives M in terms of the applied load ($2F$). An example result is shown in Fig. 9 for the case, $l = 1000$ mm, $t = 100$ mm, $B = 10$ mm, $a = 75$ mm and using the same material data as above (Fig. 2). These dimensions lead to bending stresses which are substantially larger than the shear stresses in the elastic regime. At higher loads, the bending moment falls below its elastic value due to plastic relaxation. This is because the bending moment is secondary in the sense of not being required by equilibrium alone. It is,

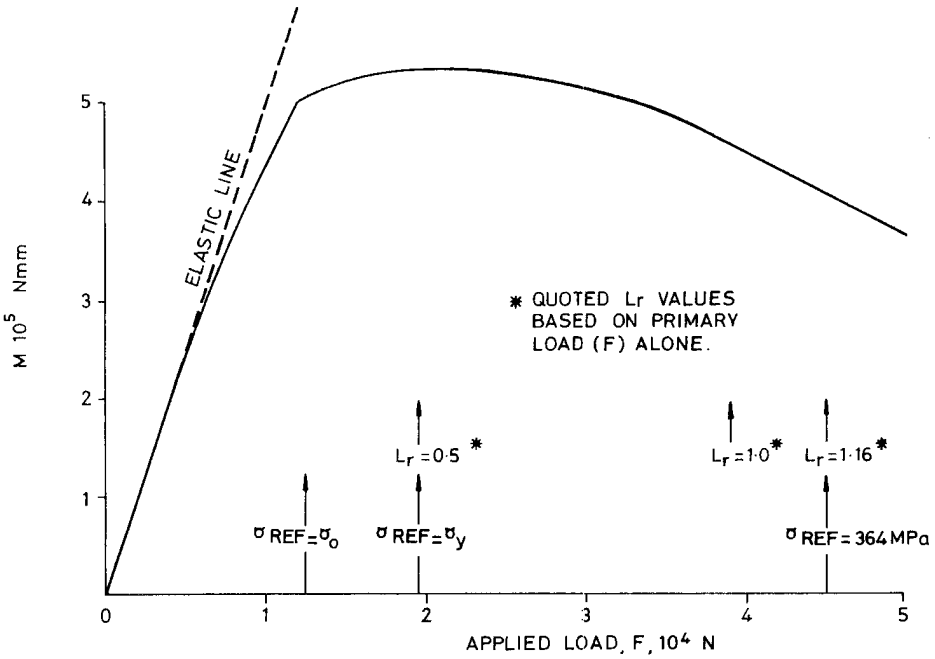

Fig. 9. Bending moment acting on ligament as a function of applied load.

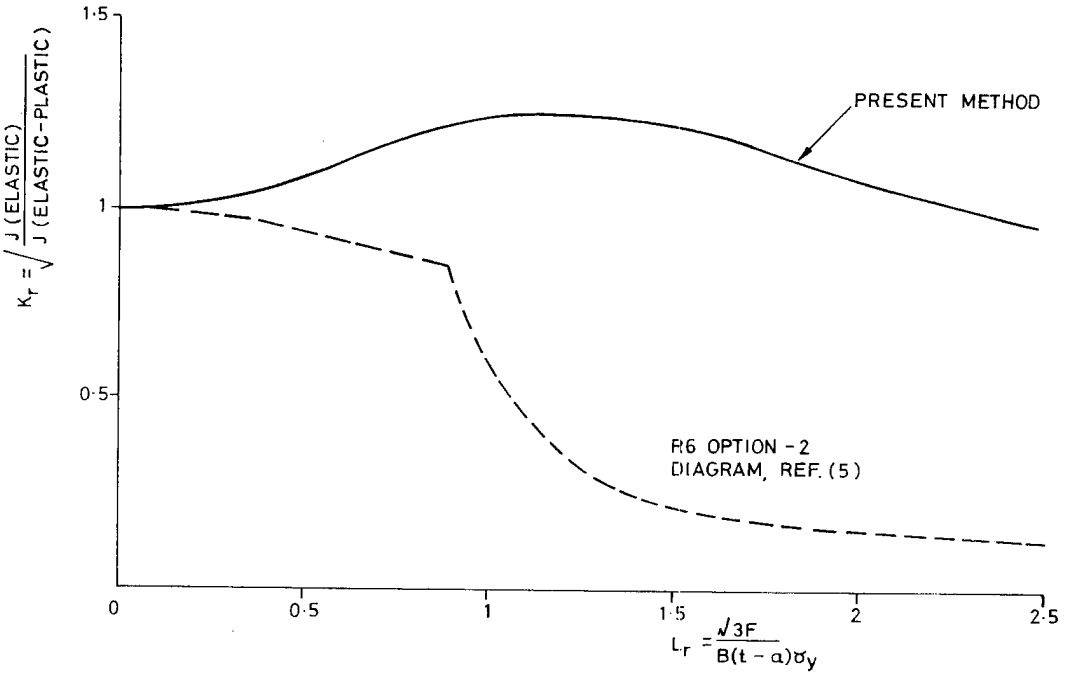

Fig. 10. Results in $R6$-format compared with 'option 2' diagram.

perhaps, surprising that relaxation occurs to the extent of leading to a decreasing moment for reference stresses greater than σ_y. However the origin of this behaviour can be seen by differentiating eq. (27), giving,

$$\frac{dM}{dF} = \frac{\alpha - B\int \frac{\partial^2 J}{\partial F \partial M} da}{\beta + B\int \frac{\partial^2 J}{\partial M^2} da}. \tag{32}$$

Although the second term in the numerator is zero elastically, in the plastic regime it is non-zero and typically increases rapidly with the reference stress. Consequently, a zero of the derivative, i.e. a maximum in M, is to be expected. However, as a caution, we note that the theory presented here applies strictly only for non-linear elasticity, i.e. reversible behaviour, and the situation may be different for truly plastic (irreversible) materials. Finally, Fig. 10 plots the normalized J in $R6$ format against the normalized applied load. For comparison the 'Option-2' R6 diagram is also shown, [5]. The difference is due to the relaxation of the (secondary) bending moment, which, for the largest applied loads becomes negligible. J is generally smaller than its elastic value, rather than being larger as would be the case for primary stressing.

CONCLUSIONS

The foregoing examples have shown that the reference stress approximation for J, (2, 3), may be employed in situations where the loading is secondary, or partly secondary, in nature. The resulting analytic procedure for estimating J is simple to use and has the advantage that it lends physical insight into the problem, unlike numerical techniques. The procedure is analogous to classical structural analysis in that the problem is first simplified by the introduction of a small number of load-resultants (e.g. shearing force and bending moment). The method should therefore appeal to practising engineers for the purposes of application.

Acknowledgements—The author is grateful to the Divisional Director, OED CEGB, for permission to publish this paper.

REFERENCES

[1] J. D. Eshelby, The energy–momentum tensor in continuum mechanics, in *The Inelastic Behaviour of Solids* (Edited by M. F. Kanninen). McGraw-Hill, NY (1970).
[2] J. R. Rice, *J. appl. Mech.* **35**, 379–386 (1968).
[3] V. Kumar, M. D. German and C. F. Shih, An Engineering Approach for Elastic–Plastic Fracture Analysis. EPRI NP-1931, July 1981.
[4] R. A. Ainsworth, The assessment of defects in structures of strain hardening materials, *Engng Fracture Mech.* **19**, 633–642 (1984).
[5] R. A. Ainsworth, A. Dowling, I. Milne and A. T. Stewart, Revision 3 of R6: its background and validity. *Proc. Fracture Control of Engineering Structures, ECS6* (Edited by H. C. Van Elst and A. Bakker), Amsterdam, (June 1986).
[6] A. Muscati, To be published.

(*Received* 8 *June* 1987)